Pure Appl. Chem., Vol. 81, No. 11, pp. 2025–2033, 2009.
doi:10.1351/PAC-CON-08-12-04

Immobilization of 5,10,15,20-tetrakis-(2-fluorophenyl)porphyrin into MCM-41 and NaY: Routes toward photodegradation of pesticides*

Monica Silva[1], Maria E. Azenha[1,‡], Mariette M. Pereira[1], Hugh D. Burrows[1], Mohamed Sarakha[2], Maria F. Ribeiro[3], Auguste Fernandes[3], Paula Monsanto[4], and Fernando Castanheira[4]

[1]Department of Chemistry, Faculty of Sciences and Technology, Coimbra University, Rua Larga, 3004-535 Coimbra, Portugal; [2]Laboratoire de Photochimie Moléculaire et Macromoléculaire, Université Blaise Pascal, 24, Avenue des Landais, 63177 Aubière, France; [3]IBB, Department of Chemical Engineering, IST, Lisbon Technical University, Av. Rovisco Pais, 1049-001 Lisbon, Portugal; [4]National Institute of Legal Medicine, Centre Branch, Department of Forensic Toxicology, Largo da Sé Nova, 3000-213 Coimbra, Portugal

Abstract: NaY zeolite and MCM-41 mesoporous molecular sieve were used as supports for immobilization of 5,10,15,20-tetrakis-(2-fluorophenyl)porphyrin (TFPP) using adsorption and ship-in-the-bottle routes involving the nitrobenzene method. The materials obtained were characterized by thermogravimetry/differential thermal analysis (TG/DTA), nitrogen adsorption, UV–vis absorption, diffuse reflectance (DRS), and luminescence spectroscopy. Although the porphyrin could easily be synthesized inside MCM-41 pores using the ship-in-the-bottle route, no significant porphyrin was formed in the smaller supercages of NaY zeolite, since the reaction stops at the dipyrrolylmethene intermediate (FDPM). Promising preliminary studies were made in the photodegradation of the pesticides, 2,3,5-trimethylphenol (TMP) and mecoprop (MCPP), using as catalyst TFPP encapsulated in mesoporous MCM-41 material. The 2-hydroxymethyl-hydroquinone and 4-chloro-2-methylphenol were identified as the main degradation products of MCPP. The encapsulated system resulting from the TFPP template synthesis shows significantly enhanced performance when compared with adsorbed porphyrin in both supports.

Keywords: immobilization; molecular sieves; pesticides; photodegradation; porphyrins.

INTRODUCTION

The demand for agricultural processes to improve food production has led to large-scale use of pesticides, which unfortunately are persistent and may cause serious long-term environmental problems. In recent decades, several studies have appeared which promote their elimination either by advanced oxidation processes or involving photodegradative routes [1,2]. Porphyrins and metalloporphyrins have

*Paper based on a presentation at the 2nd International Conference on Green Chemistry (ICGC-2), 14–20 September 2008, Moscow, Russia. Other presentations are published in this issue, pp. 1961–2129.

‡Corresponding author

been widely used as oxidative catalysts in homogenous systems, making use of peroxides or oxygen as oxidant [3–5]. There are also several reports of using porphyrins as photosensitizers for photodegradation of pollutants [5–8].

To allow large-scale application and reuse of porphyrins or metalloporphyrins, they need to be immobilized into organic or inorganic solids. Various supports have been studied for this, such as modified silica surfaces [9,10], zeolites [11], organic polymers [12,13], cyclodextrins [14], and membranes [15].

Although zeolites and mesoporous materials have the appropriate structure for use in the adsorption and/or ship-in-the-bottle encapsulation of porphyrins, their use for the immobilization of porphyrins has not been significantly exploited [4,11,16–18] as seen in a recent review by Derouane [19]. To the best of our knowledge, there are no publications of application of these systems in the sensitized photodegradation of pesticides by visible light in the solar wavelength range.

In this paper, we report the immobilization of 5,10,15,20-tetrakis-(2-fluorophenyl)porphyrin (TFPP) in NaY and MCM-41, using adsorption or in situ porphyrin synthesis (ship-in-the-bottle) using nitrobenzene methodology [20]. Some structural characterization of immobilized TFPP has been made using combined thermogravimetry/differential thermal analysis (TG/DTA) and nitrogen adsorption measurements, UV–vis absorption, diffuse reflectance (DRS), and luminescence spectroscopies. This immobilized porphyrin has been tested as photocatalyst for photodegradation of two pesticides, 2,3,5-trimethylphenol (TMP) and mecoprop (MCPP). The evolution of the reaction was followed using UV–vis absorption spectroscopy, and high-performance liquid chromatography (HPLC) and some of the photoproducts were identified using gas chromatography-mass spectrometry (GC-MS) analysis.

EXPERIMENTAL

Materials and methods

MCPP [2-(4-chloro-*o*-tolyloxy)propionic acid], 95 % purity, was purchased from Aldrich, and TMP, >98 % purity, was purchased from Fluka. All the standards were from Fluka and Aldrich and were of the highest grade available. They were used as received. The solvents were purified by standard methods and the other reagents used as provided. The solutions were prepared with deionized ultrapure water, which was obtained with a Milli-Q device (Millipore). The zeolite NaY and the mesoporous MCM-41 were purchased from Zeolyst and Aldrich, respectively, and pretreated at 500 °C for 18 h in an oven. TFPP was obtained using the nitrobenzene method, as described in the literature [20]. In homogeneous synthesis, the porphyrin was obtained as violet crystals (yield = 25 %), and the characterization was done by UV–vis absorption and luminescence spectroscopy that is in agreement with previously reported data [21].

The dipyrrolylmethene (FDPM) was obtained by reacting the pyrrole with 2-fluorobenzaldehyde with a residual amount of glacial acetic acid, at 120 °C during 1 h. In this synthesis, FDPM was obtained as brown crystals.

Instrumentation

UV–vis absorption spectra of solution samples were measured on a Shimadzu UV-2010 double-beam spectrometer over the range 200–800 nm. The thermogravimetry/differential thermal analysis (TG/DTA) studies were carried out using SETARAM-TG/DTA 92 equipment under air atmosphere to a maximum temperature of 900 °C, with a heating rate of 10 °C min^{-1}. UV–vis diffuse reflectance spectra (DRS) were obtained at room temperature, over the wavelength range 250–800 nm, using a Cary 5000 spectrophotometer with Spectralon as standard. Luminescence spectra were made on a SPEX Fluorolog 3-22 spectrophotometer, in the UV–vis range, with a 300 W xenon arc lamp as excitation

source. The luminescence spectra were made using a specially designed metal support with a quartz window.

Analysis of degradation products of TMP and MCPP was followed by HPLC using a Hewlett Packard system (HP1050) equipped with a UV–vis photodiode array detector with detection set at 270 nm for both compounds. A reverse-phase Merck column (Spherisorb ODS-2, 5 μm) was used with a mixture of water (0.1 % formic acid) and acetonitrile (60:40 v/v) as eluent in isocratic mode with a flow rate of 1.0 ml min^{-1}. The GC-MS analysis of the final photoproducts were carried out in an Agilent 6890 GC System Plus +, equipped with an autosampler and a split/splitless injector operated in the split mode. The injector was kept isothermally at 240 °C. Analytes were separated using an HP-5MS column (30 m × 0.32 mm i.d. and 0.25-μm film thickness). Helium was used as carrier gas. The oven temperature program was: 120 °C for 2.0 min, then ramped to 240 °C at 5 °C min^{-1}, to 270 °C at 30 °C min^{-1}, and held for 10 min. The total run time was 27 min. The gas chromatograph was coupled to an Agilent 5973 mass selective detector with electron impact mode, operated in the SIM mode. The interface temperature was maintained at 280 °C.

Immobilization of TFPP in MCM-41 and NaY

After consideration of the various possibilities suggested for incorporating porphyrins and metalloporphyrins inside the pores or cavities of microporous and mesoporous materials [16], two basic approaches were used for entrapping TFPP inside the MCM-41 and NaY materials: (i) the adsorption method; and (ii) the ship-in-the-bottle synthesis.

Adsorption method (TFPPadsMCM-41 and TFPPadsNaY)

Typically, 2.0 g of MCM-41 and NaY were mixed with 20 ml of a CH_2Cl_2 porphyrin solution (5×10^{-6} mol l^{-1}) which was then stirred for 3 h at 21 °C. The final material was filtered and washed repeatedly with CH_2Cl_2 until no free porphyrin was detected in the solution by UV–vis spectroscopy. Two materials were obtained, a pale beige solid consisting of TFPP anchored in NaY (TFPPadsNaY) and a pale green solid of TFPP anchored in MCM-41 (TFPPadsMCM-41). These solids were dried overnight at 100 °C.

Template synthesis method (ship-in-the-bottle) (TFPP@MCM-41 and FDPM@NaY)

In a typical experiment, 2.0 g of MCM-41 and NaY were refluxed with pyrrole and 2-fluorobenzaldehyde in the presence of glacial acetic acid and nitrobenzene, at 120 °C. After 1.5 h, the rose colored sample with NaY and the intense brown sample with MCM-41 were filtered and the resulting materials were Soxhlet extracted sequentially with CH_2Cl_2, CH_3CN, and $CHCl_3$, until no excess of porphyrin and/or precursors was detected in the solution. The resulting immobilized sensitizers were dried overnight at 100 °C.

General procedure for photodegradative experiments

TFPP@MCM-41 (5 mg) was added to 25 ml of an aqueous solution of MCPP (5×10^{-4} mol l^{-1}) and TMP (5×10^{-4} mol l^{-1}) at pH ≅ 6. The process was carried out at 23 °C in a Pyrex tubular reactor, with external water cooling, with the upper end of the reactor open to the atmosphere. The suspensions were stirred vigorously and irradiated with three medium-pressure mercury lamps 125 W. The suspensions were centrifuged, and the liquid phase was filtered to remove the catalyst. The reaction was monitored by UV–vis spectroscopy (λ = 280 nm) and HPLC, at regular times, and the photoproducts were identified by GC-MS after extraction with dichloromethane and ethyl acetate. The preliminary results with the other catalysts are not described.

RESULTS AND DISCUSSION

Immobilization of porphyrins in MCM-41 and NaY

To immobilize TFPP in MCM-41 and NaY, we used two different procedures: (i) adsorption of a presynthesized halogenated porphyrin (TFPP), and (ii) ship-in-the-bottle synthesis, involving the condensation–cyclization and oxidation of pyrrole with 2-fluorobenzaldehyde inside a porous material, using the nitrobenzene method.

In the first approach, the porous materials (MCM-41 and NaY) were added to a dichloromethane solution of TFPP and kept with stirring during 3 h, at room temperature. After this period, the solid was filtered and washed again with dichloromethane to remove excess of porphyrin.

For the ship-in-the-bottle synthesis, two preferred methods have been presented in the literature for the one-pot synthesis of *meso*-arylporphyrins: (i) the Adler method [22] that promotes the condensation of pyrrole with arylaldehydes in propionic acid followed by oxidation of the porphyrinogen with oxygen, and (ii) the nitrobenzene method [20] that promotes the condensation–oxidation of pyrrole with arylaldehydes in acetic acid/nitrobenzene, directly. The latter method has the advantage of producing the pure porphyrin without any contamination from the corresponding chlorines, as is always observed with Adler's synthetic method.

For this synthesis, equimolar amounts of pyrrole and 2-fluorobenzaldehyde, dissolved in acetic acid and nitrobenzene, were refluxed during 1.5 h, in the presence of previously dehydrated porous materials. After filtration, the modified materials were submitted to Soxhlet extraction, using sequentially different solvents (CH_2Cl_2, CH_3CN, and $CHCl_3$) to remove excess of adsorbed materials. The solids obtained by both synthetic methods were dried and characterized as described below.

Characterization of the immobilized sensitizers

UV–vis absorption and luminescence spectroscopy

The UV–vis absorption and luminescence spectra of the recovered TFPP obtained after the cyclization–oxidation reaction in the presence of MCM-41 from methanol solution are presented in Fig. 1. The general structure of these spectra is in agreement with that described in the literature [21].

The UV–vis absorption spectrum of TFPP in methanol solution (Fig. 1a) shows the typical Soret band (411 nm) and four Q bands (512, 550, 580, and 632 nm) attributed to the (0,0) and (0,1) vibronic progression of the Q_x and Q_y bands [23]. The luminescence spectrum presents two intense bands at 655 and 710 nm (Fig. 1b).

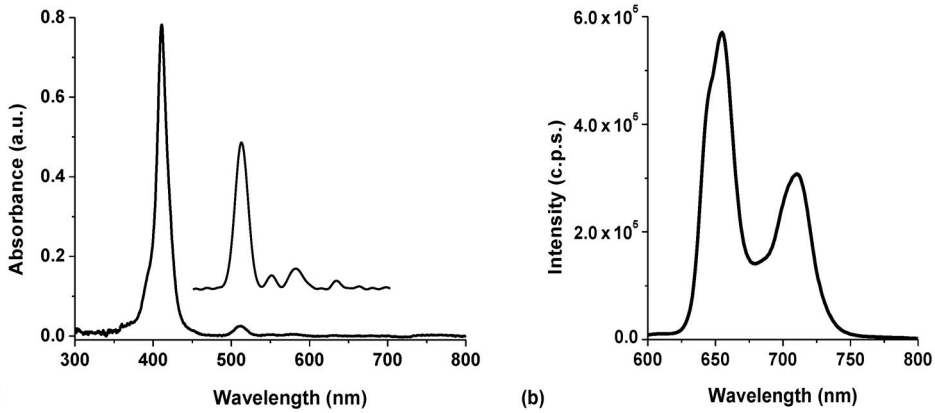

Fig. 1 (a) UV–vis absorption spectrum (insert: region 450–700 nm expanded to see the Q bands); (b) luminescence spectra of TFPP in methanol (5×10^{-6} mol l^{-1}). The excitation wavelength was 411 nm (Soret band).

The emission spectra of TFPP@MCM-41 and TFPPadsMCM-41 are presented in Figs. 2a and 2b, respectively. The shape of the solid TFPP@MCM-41 spectrum is in general agreement with that observed in solution (Fig. 1b). However, it should be noticed that the fluorescence spectrum of TFPPadsMCM-41 presents a blue shift with considerable broadening. These differences in the fluorescence spectrum are probably due to the coexistence of different porphyrin environments in the supports.

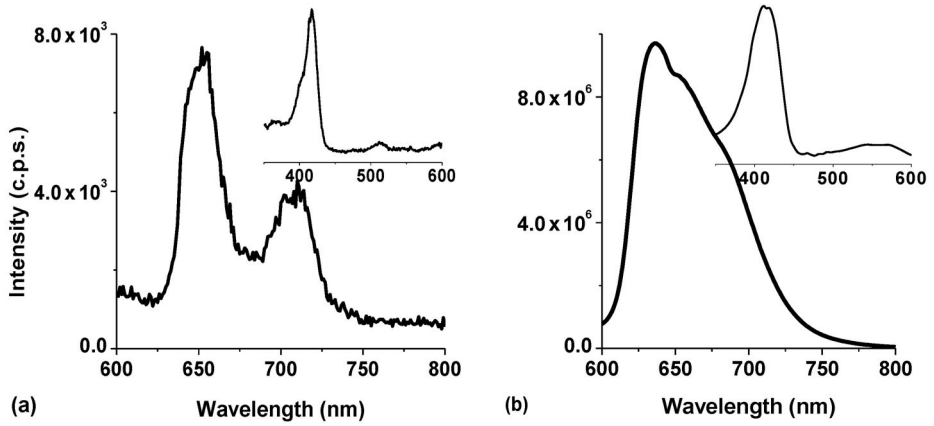

Fig. 2 Luminescence emission spectra of the (a) TFPP@MCM-41, and (b) TFPPadsMCM-41. Insert: luminescence excitation spectra.

The excitation spectra of TFPP@MCM-41 and TFPPadsMCM-41 (insert spectra, Fig. 2) are in agreement with the absorption spectrum of the TFPP in solution, which is indicative of the presence of porphyrin in the support MCM-41 prepared by both synthetic procedures.

The emission spectra of FDPM@NaY and TFPPadsNaY are presented in Figs. 3a and 3b, respectively. The emission spectra of FDPM@NaY shows broad bands with maximum at 670 nm, while the emission of TFPPadsNaY shows two typical bands (651 nm; 710 nm), similar to those observed in homogeneous solution. The excitation spectra of FDPM@NaY (insert spectrum, Fig. 3a) does not correspond to that of a typical porphyrin absorption spectra, while in contrast that of TFPPadsNaY (insert spectrum, Fig. 3b) is similar to the absorption spectra of the porphyrin in homogeneous solution.

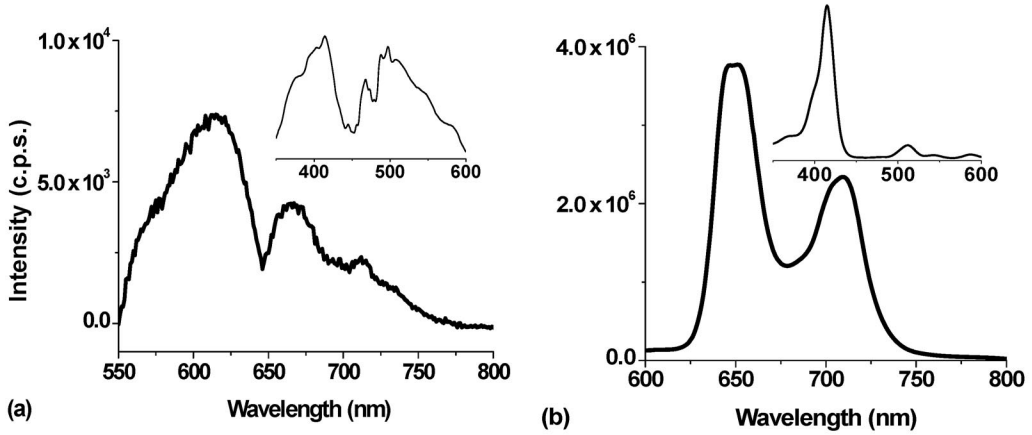

Fig. 3 Luminescence emission spectra of the (a) FPDM@NaY, and (b) TFPPadsNaY. Insert: luminescence excitation spectra.

UV–vis DRS spectroscopy

Figure 4 presents UV–vis DRS spectra of the immobilized sensitizers TFPPadsMCM-41 (Fig. 4a), TFPP@MCM-41 (Fig. 4b), TFPPadsNaY (Fig. 4c), and FDPM@NaY (Fig. 4d), over the range 300–700 nm.

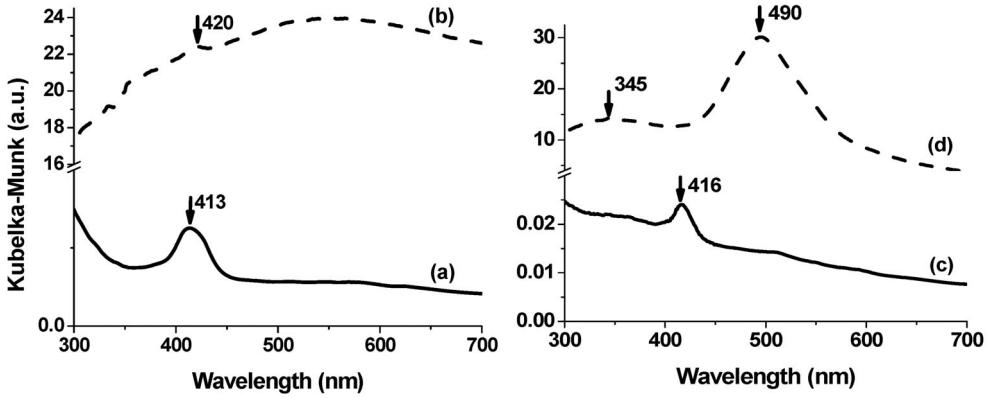

Fig. 4 DRS of the (a) TFPPadsMCM-41; (b) TFPP@MCM-41; (c) TFPPadsNaY; (d) FDPM@NaY.

The DRS of TFPPadsMCM-41 (Fig. 4a) and TFPPadsNaY (Fig. 4c) show intense bands at about 415 nm, typical of the Soret band of the UV–vis absorption spectra of porphyrin in homogeneous solutions. The low intensity of the Q bands may possibly result from the effect of light scattering.

In the TFPP@MCM-41 spectrum (Fig. 4b) the Soret band is seen at 420 nm, together with a broad band centered at 550 nm, while with FDPM@NaY (Fig. 4d) there is no absorption band within the typical Soret region, but instead a single broad band is observed at 490 nm.

The differences between the absorption and the excitation spectra of the material from the ship-in-the-bottle synthesis in NaY, as well as the fact that in the DRS no Soret band is observed, clearly indicates that no significant synthesis of the porphyrin macrocycle occurs in the cavity of the NaY zeolite. This is in agreement with the fact that the size of *meso*-porphyrins (ca. 18.44 Å) are too large to fit within the NaY supercage (ca. 12 Å). In contrast, they can easily be included inside the MCM-41 channels (ca. 30 Å).

The broad band at 490 nm is attributed to the formation of the porphyrin precursor, FDPM, synthesized by direct condensation of 2-fluorobenzaldehyde in pure pyrrole, which presents an identical absorption band. This is in good agreement with a previous study described by Garcia et al. [18].

TG analysis and surface area

TG analysis shows that the immobilized porphyrin material is stable up to 350 °C (Fig. 5). The first weight loss occurs at 100–150 °C, is slightly endothermic, and corresponds to the loss of adsorbed water weakly bound to the support. The next decomposition occurs at 390 and 550 °C in MCM-41 and at 450 and 540 °C in NaY, and is due to the degradation of the immobilized materials. Weight losses were obtained of 14 % (w/w) for TFPP@MCM-41 and 12 % (w/w) for FDPM@NaY. The TG analysis of the samples TFPPadsMCM-41 and TFPPadsNaY did not show significant weight losses above 200 °C (< 2 % (w/w)), and is not shown.

The surface areas (BET analysis) in TFPP@MCM-41 and FDPM@NaY show decreases of 23 and 50 %, respectively, compared to the bare supports MCM-41 and NaY. The samples obtained by the adsorption process, TFPPadsMCM-41 and TFPPadsNaY, showed a surface area decrease of about

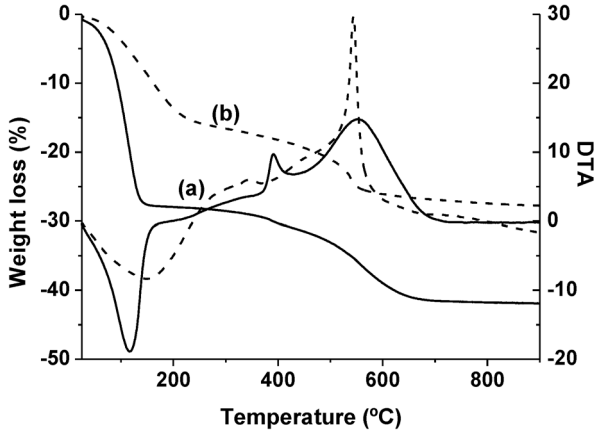

Fig. 5 TG/DTA analyses of the (a) TFPP@MCM-41; (b) FDPM@NaY.

10 % and the pore volume reduces to almost zero. These results indicate that the immobilization of the porphyrin is dependent on the synthetic method. Using the ship-in-the-bottle procedure, the porphyrin is located predominantly inside the pores of the support MCM-41, while when it was immobilized via adsorption route it is mainly in the external surface of MCM-41 or NaY.

Photodegradation experiments

TFPP immobilized on MCM-41 and NaY, by the methods described above, showed photoactivity in the degradation of TMP and MCPP. The most promising results were obtained using TFPP@MCM-41.

Figures 6 and 7 present the photodegradation of TMP and MCPP, respectively, followed by HPLC, using TFPP@MCM-41 and the MCM-41 support, that shows the photoactivity of the porphyrin immobilized compared with the bare support. The photodegradation was almost 75 % after 3 h for both pesticides.

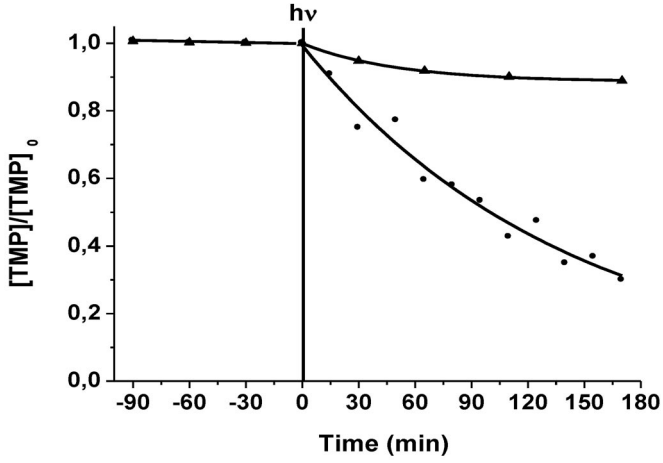

Fig. 6 TMP/TMP_0 ratio vs. irradiation time in the presence of (▲) MCM-41; (●) TFPP@MCM-41.

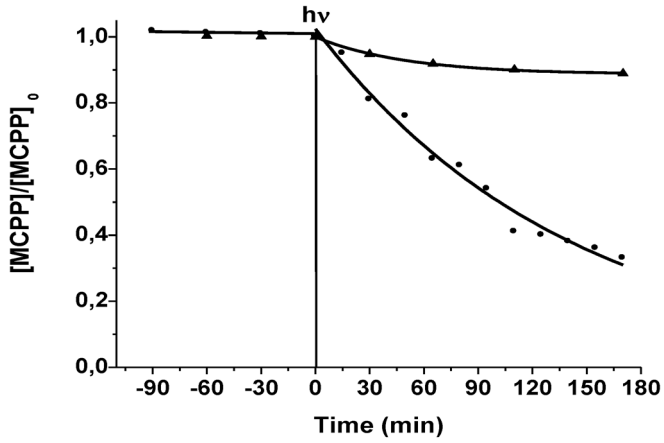

Fig. 7 MCPP/MCPP$_0$ ratio vs. irradiation time in the presence of (▲) MCM-41; (●) TFPP@MCM-41.

The sensitized photodegradation of MCPP and TMP was observed using TFPP@MCM-41 with conversions about 50 % after 90 min. Several photoproducts were observed, and the characterization of all photoproducts and the mechanistic studies are underway and will be presented in another paper. We note, however, using GC-MS the formation of 2-hydroxymethyl-hydroquinone (M^+ = 140) and 4-chloro-2-methylphenol (M^+ = 142), as the main photoproducts for MCPP photodegradation.

CONCLUSIONS

TFPP has been immobilized on the supports MCM-41 and NaY by adsorption and incorporated in MCM-41 by ship-in-the-bottle synthesis. This latter route is not possible with NaY due to the pores being smaller than the size of the porphyrin. The systems have been tested as photosensitizers for the degradation of the pesticide MCPP and the model system TMP. In both cases, efficient degradation is observed, suggesting that these systems may provide a viable route to catalyze the photodegradation of pesticides.

ACKNOWLEDGMENTS

We thank Fundação para a Ciência e a Tecnologia (FCT) for financial support through the project PTDC/QUI/66015/2006, and GRICES for the collaboration between Coimbra and Clermont Ferrand through the Programme PESSOA 2007-2008. M. E. Azenha thanks CNRST-MAROC-GRICES for support throughout the bilateral program Proc.º4.1.5/CNRST/Marrocos/2008. M. Silva also thanks FCT for a post-doc grant SFRH/BPD/34372/2007.

REFERENCES

1. H. D. Burrows, M. Canle L., J. A. Santabella, S. Steenken. *J. Photochem. Photobiol. B: Biol.* **67**, 71 (2002).
2. O. Legrini, E. Oliveros, A. M. Braun. *Chem. Rev.* **93**, 671 (1993).
3. (a) B. Meunier. *Chem. Rev.* **92**, 1411 (1992); (b) B. Meunier. In *Metalloporphyrins Catalyzed Oxidations*, F. Montanari, L. Casella (Eds.), Chap. 1, Kluwer Academic, Dordrecht (1994).
4. H. Nur, H. Hamid, S. Endud, H. Hamdan, Z. Ramli. *Mater. Chem. Phys.* **96**, 337 (2006).
5. S. L. H. Rebelo, M. M. Pereira, P. V. Monsanto, H. D. Burrows. *J. Mol. Catal. A: Chem.* **297**, 35 (2009).

6. E. Silva, M. M. Pereira, H. D. Burrows, M. E. Azenha, M. Sarakha, M. Bolte. *Photochem. Photobiol. Sci.* **3**, 200 (2004).
7. C. J. P. Monteiro, M. M. Pereira, M. E. Azenha, H. D. Burrows, C. Serpa, L. G. Arnaut, M. J. Tapia, M. Sarakha, P. Wong-Wah-Chung, S. Navaratnam. *Photochem. Photobiol. Sci.* **4**, 617 (2005).
8. D. Murtinho, M. Pineiro, M. M. Pereira, A. M. d'A. Rocha Gonsalves, L. G. Arnaut, M. G. Miguel, H. D. Burrows. *J. Chem. Soc., Perkin Trans. 2* 2441 (2000).
9. P. R. Cooke, J. R. Lindsay Smith. *J. Chem. Soc., Perkin Trans. 1* 1913 (1994).
10. F. S. Vinhado, P. R. Martins, A. P. Masson, D. G. Abreu, E. A. Vidoto, O. R. Nascimento, Y. Iamamoto. *J. Mol. Catal. A: Chem.* **188**, 141 (2002).
11. F. Bedioui. *Coord. Chem. Rev.* **144**, 39 (1995).
12. D. Pattou, G. Labat, S. Defrance, J. L. Séris, B. Meunier. *New J. Chem.* **13**, 801 (1989).
13. A. V. Borissov, V. I. Tsivenko, I. A. Myasnikov. *Zh. Fiz. Khim.* **63**, 2540 (1991).
14. Y. Kuroda, T. Sera, H. Ogoshi. *J. Am. Chem. Soc.* **113**, 2793 (1991).
15. C. C. Warmser, M. Calvin, G. A. Graf. *J. Membr. Sci.* **28**, 31 (1986).
16. V. Radha Rani, M. Radha Kishan, S. J. Kulkarni, K. V. Rughavan. *Catal. Commun.* **6**, 531 (2005).
17. D. Srinivas, S. Sivasanker. *Catal. Surv. Asia* **7**, 121 (2003).
18. F. Algarra, M. A. Esteves, V. Fornés, H. Garcia, J. Primo. *New J. Chem.* 333 (1998).
19. E. G. Derouane. In *Catalysts for Fine Chemical Synthesis: Microporous and Mesoporous Solid Catalysts*, E. G. Derouane (Ed.), Vol. 4, p. 216, John Wiley, Chichester (2006).
20. A. M. d'A Rocha Gonsalves, J. M. T. B. Varejão, M. M. Pereira. *J. Heterocycl. Chem.* **28**, 635 (1991).
21. C. J. P. Monteiro, M. M. Pereira, S. M. A. Pinto, A. V. C. Simões, G. F. F. Sá, L. G. Arnaut, S. J. Formosinho, S. Simões, M. F. Wyatt. *Tetrahedron* **64**, 5132 (2008).
22. A. D. Adler, F. R. Longo, F. Kampas, J. Kim. *J. Inorg. Nucl. Chem.* **32**, 2443 (1970).
23. M. Gouterman. *J. Mol. Spectrosc.* **6**, 138 (1961).